J|A|C|S ARTICLES

Published on Web 07/22/2009

Multiple Core−Shell Functionalized Colloidal Mesoporous Silica Nanoparticles

Valentina Cauda, Axel Schlossbauer, Johann Kecht, Andreas Zürner, and Thomas Bein*

Department of Chemistry and Biochemistry and Center for NanoScience (CeNS), University of Munich (LMU), Butenandtstrasse 5-13 (E), 81377 Munich, Germany

Received November 30, 2008; E-mail: bein@lmu.de

Abstract: The selective functionalization of the inner and outer surfaces of colloidal mesoporous silica (CMS) nanoparticles with different trialkoxysilanes, following a newly developed delayed co-condensation approach, results in bifunctional CMS. Complementary CMS nanoparticles were prepared with two different functional groups located either on the outer shell or in the inner core of the particle. The identification and localization of the functional groups was achieved by means of different techniques including zeta potential, nitrogen sorption measurements, and fluorescence spectroscopy. This last technique was applied to fluorescein isothiocyanate (FITC)-labeled CMS featuring aminopropyl functional groups on the periphery or the internal pore surface of the particles. Fluorescence quenching experiments were carried out with dodecanethiolate-stabilized gold nanoparticles having a diameter greater than the pore size of the CMS. It could be shown that fluorescence quenching occurs only when the FITC is positioned on the outer surface of the CMS nanoparticles, whereas no quenching was observed for FITC located in the inner core of the nanoparticle. These results clearly confirm the controlled localization of the aminopropyl groups in the nanometer space of the CMS particles. Our approach thus offers the opportunity to synthesize, in a novel multistep co-condensation strategy, various bifunctional mesoporous nanoparticles with controlled localization of different functional groups in the inner core or on the outer shell of the nanoparticle.

1. Introduction

Multiple molecular functionalities in different spatial regions of mesoporous nanoparticles are of great interest for enhancing their capabilities and performance in diverse fields such as controlled drug delivery, complex catalytic systems, and chemical sensing.

The synthesis of colloidal mesoporous silica (CMS) using surfactants leads to nanoparticles ranging in size from about 15 to 300 nm and featuring a large internal surface area and pore volume. Such nanoparticles exhibit interesting magnetic,[1] molecular sieving,[2] and molecule adsorption and controlled release[3,4] properties. Different synthetic approaches have been reported to obtain nanoscopic mesoporous silica particles. Mann and co-workers[5] used a quenching procedure for the template-directed alkaline synthesis of MCM-41 silica, neutralizing the pH of the synthesis batch by dilution with excess water and then decreasing the reaction rate. Cai et al.[6] synthesized colloidal MCM-41 silica in extremely diluted aqueous reaction mixtures, obtaining spherical particles about 110 nm in size. Recently a procedure to obtain mesoporous nanoparticles with sizes ranging from 100 nm to 1 μm was developed from an aqueous solution of sodium metasilicate and cationic surfactant.[7] Some of us have previously reported on the synthesis of CMS with tunable narrow particle size distributions using the polyalcohol triethanolamine.[8]

Moreover, the synthesis of functionalized CMS has been achieved,[9,10] and we have reported first steps regarding the control of the distribution of functionality on the inner or outer surface of such nanoparticles.[11]

Achieving controlled localization of two or more different molecular functionalities on the inner and outer surfaces of mesoporous silica nanoparticles of about 100 nm diameter would offer several profound advantages in drug delivery and other applications. The functionalization of the external surface would play an important role in tuning the interactions with the environment, such as labeling the nanoparticle with specific groups for tumor cell targeting or attaching large molecules for pore gating.[12−15] On the other hand, a different internal

(1) Giri, S.; Trewyn, B. G.; Stellmaker, M. P.; Lin, V. S.-Y. *Angew. Chem., Int. Ed.* **2005**, *44*, 5038–5044.
(2) Vartuli, J. C.; Shih, S. S.; Kresge, C. T.; Beck, J. S. *Stud. Surf. Sci. Catal.* **1998**, *117*, 13–21.
(3) Trewyn, B. G.; Giri, S.; Slowing, I. I.; Lin, V. S.-Y. *Chem. Commun.* **2007**, *31*, 3236–3245.
(4) Slowing, I. I.; Vivero-Escoto, J. L.; Wu, C.-W.; Lin, V. S.-Y. *Adv. Drug Delivery Rev.* **2008**, *60*, 1278–1288.
(5) Fowler, C. E.; Khushalani, D.; Lebeau, B.; Mann, S. *Adv. Mater (Weinheim, Ger.)* **2001**, *13*, 649–652.
(6) Cai, Q.; Luo, Z.-S.; Pang, W.-Q.; Fan, Y.-W.; Chen, X.-H.; Cui, F.-Z. *Chem. Mater.* **2001**, *13*, 258–263.
(7) Rathousky, J.; Zukalova, M.; Kooyman, P. J.; Zukal, A. *Colloids Surf. A* **2004**, *241*, 81–86.
(8) Möller, K.; Kobler, J.; Bein, T. *Adv. Funct. Mater.* **2007**, *17*, 605–612.
(9) Kobler, J.; Möller, K.; Bein, T. *ACS Nano* **2008**, *2*, 791–799.
(10) Möller, K.; Kobler, J.; Bein, T. *J. Mater. Chem.* **2007**, *17*, 624–631.
(11) Kecht, J.; Schlossbauer, A.; Bein, T. *Chem. Mater.* **2008**, *20*, 7207–7214.
(12) Park, C.; Kyoungho, O.; Lee, S. C.; Kim, C. *Angew. Chem., Int. Ed.* **2007**, *46*, 1455–1457.

functionalization could be used to adjust the molecular interactions of specific cargo molecules with the internal surface of the mesoporous nanoparticle, thus controlling diffusional transport and delivery kinetics as well as the stability of the biologically active molecules.[16−18]

Different strategies have recently been developed to selectively functionalize the internal and external surfaces of bulk mesoporous silica materials. Cheng et al.[19] illustrated the differential functionalization of mesoporous silica spheres with 9-fluorenylmethyloxycarbonyl (Fmoc)-protected alkylamines, which can be selectively activated by diffusion-based cleavage using a solution of piperidine in DMF. Other authors followed a multistep procedure, first functionalizing the external surface of template-filled as-synthesized MCM-41 and, after template extraction, grafting a different organic group in the interior of the pores.[20] We emphasize that this approach can only be used effectively with micrometer-sized silica materials, because template-filled mesopores still permit diffusion of grafting agents, albeit more slowly. Thus, in mesoporous nanoparticles, spatial selectivity cannot be easily achieved with this strategy. Furthermore, in some cases, the surfactant can be replaced by functionalized organosiloxanes.[21,22]

In an effort to achieve a greater control over the amount and density of the functional groups in CMS nanoparticles, some of us have previously reported a new site-selective co-condensation approach that permits us to selectively control the functionalization of the outer versus the internal pore surface.[11]

In the present work, we report on the synthesis of CMS having two different functional groups on the inner surface and on the outer shell of the particles (Figure 1). Following the already reported synthetic procedure using the polyalcohol triethanolamine,[8] non-aggregated colloidal suspensions of CMS were obtained. A novel delayed co-condensation protocol controlling the co-condensation of silica precursors at different stages of particle growth allows us to selectively functionalize, with two different trialkoxysilanes, the inner core and the outer shell of the CMS (Figure 1).

The prepared samples were characterized by different techniques, including nitrogen sorption measurements, transmission electron microscopy (TEM), scanning electron microscopy (SEM), dynamic light scattering (DLS), and thermogravimetric analysis (TGA). The analysis of the zeta potential of particles having aminopropyl groups in the inner or outer surface provided a clear indication of the position of the functional groups. The key issue of the spatial distribution and localization of the different functional groups was addressed with selective fluorescence quenching of covalently attached fluorescein isothiocyanate (FITC) by means of external gold nanoparticles that can only interact with external molecular moieties. As we will show in this article, the delayed co-condensation synthesis indeed provides an effective strategy for placing different molecular functionalities at different locations in the mesoporous nanoparticles.

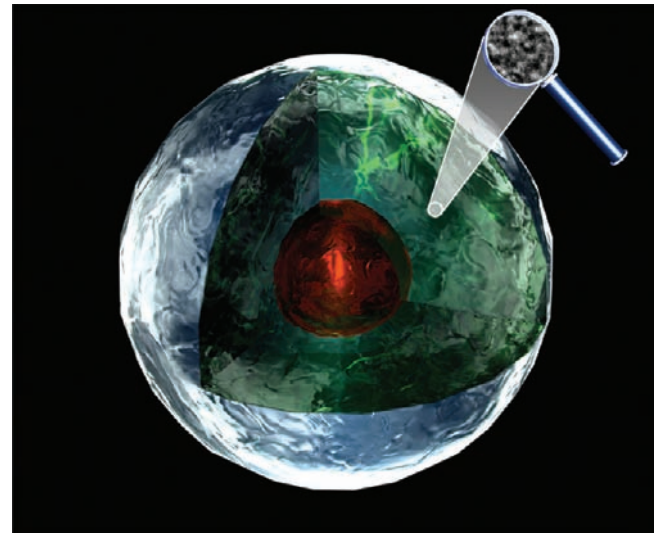

Figure 1. Artist's concept of a core−shell mesoporous silica nanoparticle, having two different functional groups in the inner core (red) and on the outer shell (blue), separated by an unfunctionalized silica layer (green).

2. Experimental Section

2.1. Synthesis of CMS by Co-condensation + Post-grafting: Approach A. A mixture of 14.3 g (95.6 mmol) of triethanolamine (TEA, Aldrich, 98%) and 1.92 g (9.22 mmol) of tetraethyl orthosilicate (TEOS, Fluka, >98%) was heated for 20 min at 90 °C without stirring in a 100 mL polypropylene reactor (solution 1). Meanwhile, a mixture of 2.41 mL (7.29 mmol) of cetyltrimethylammonium chloride (CTAC, Fluka) and 21.7 g (1.21 mol) of bidistilled water from a Millipore system (Milli-Q Academic A10) (solution 2) was heated at 60 °C and then added to solution 1. The resulting mixture, having a molar composition of 1 TEOS:0.20 CTAC:10.4 TEA:130.2 H_2O, was then stirred at 500 rpm for 30 min (Figure 2a, first step). After that time, the functionalized trialkoxysilane (RTES) reagent, acting as outer-surface-functionality, was added in combination with TEOS, with the molar ratio RTES:TEOS of 1:1 (Figure 2a, second step). The amount of RTES added corresponds to 1% (0.0922 mmol) of the initial amount of TEOS, as used in solution 1. Notwithstanding that this amount is sufficient for a complete functionalization of the outer particle surface, to achieve a higher density of functionalization, the amount of RTES was also doubled (2%, 0.184 mmol), while maintaining the ratio RTES:TEOS equal to 1.

The RTES reagents used here were (3-chloropropyl)trimethoxysilane (Cl-PTES, Fluka, 98%) and (3-aminopropyl)trimethoxysilane (APTES, ABCR, 96%) for samples CMS(A)-Cl_{OUT} and CMS(A)-NH_{OUT}, respectively.

If no outer functionalization was intended, the reaction mixture of solution 1 + 2 was left to stir overnight at room temperature (unfunctionalized CMS, named Un-CMS).

After addition of 100 mL of ethanol, the outer-functionalized or unfunctionalized CMS nanoparticles were separated by centrifugation (19.000 rpm, 43.146 RCF, 20 min), redispersed in ethanol, and extracted according to the procedure described below.

(13) Lin, Y.-S.; Tsai, C. P.; Huang, H. Y.; Kuo, C. T.; Hung, Y.; Huang, D. M.; Chen, Y. C.; Mou, C. Y. *Chem. Mater.* **2005**, *17*, 4570–4573.
(14) Lai, C. Y.; Trewyn, B. G.; Jeftinija, D. M.; Jeftinija, K.; Xu, S.; Jeftinija, S.; Lin, V. S.-Y. *J. Am. Chem. Soc.* **2003**, *125*, 4451–4459.
(15) Slowing, I. I.; Trewyn, B. G.; Lin, V. S.-Y. *J. Am. Chem. Soc.* **2006**, *128*, 14792–14793.
(16) Manzano, M.; Aina, V.; Arean, C. O.; Balas, F.; Cauda, V.; Colilla, M.; Delgado, M. R.; Vallet-Regí, M. *Chem. Eng. J.* **2008**, *137*, 30–37.
(17) Rosenholm, J. M.; Linden, M. *J. Controlled Release* **2008**, *128*, 157–164.
(18) Yang, Q.; Wang, S.; Fan, P.; Wang, L.; Di, Y.; Lin, K.; Xiao, F.-S. *Chem. Mater.* **2005**, *17*, 5999–6003.
(19) Cheng, K.; Landry, C. C. *J. Am. Chem. Soc.* **2007**, *129*, 9674–9685.
(20) De Juan, F.; Ruiz-Hitzky, E. *Adv. Mater. (Weinheim, Ger.)* **2000**, *12*, 430–432.
(21) Antochshuk, V.; Araujo, A. S.; Jaroniec, M. *J. Phys. Chem. B* **2000**, *104*, 9713–9719.
(22) Bourlinos, A. B.; Karakostas, T.; Petridis, D. *J. Phys. Chem. B* **2003**, *107*, 920–925.

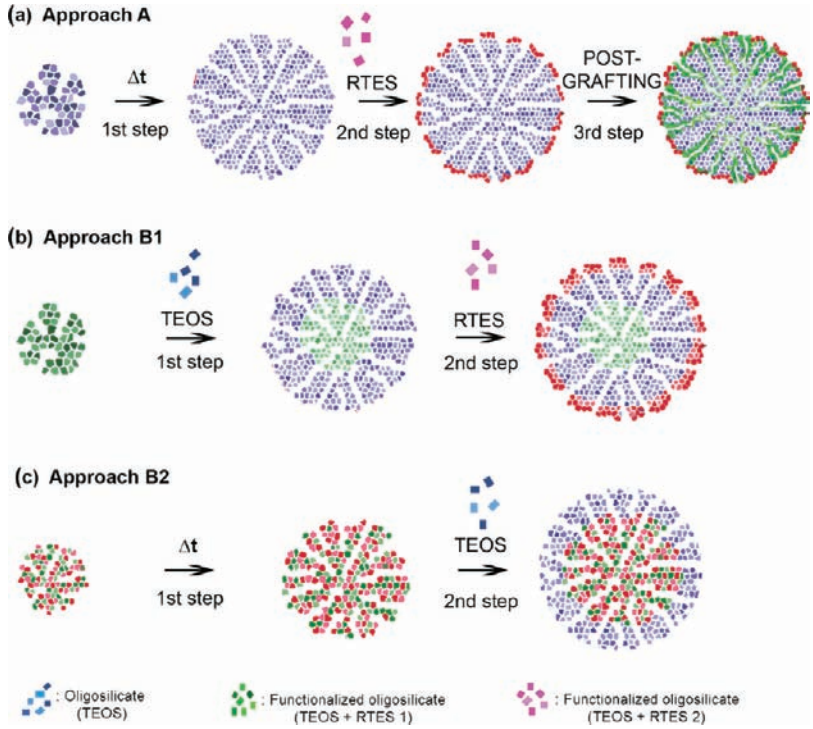

Figure 2. Scheme of the two synthetic approaches used to achieve the bifunctionalization of the core−shell nanoparticles. (a) In approach A, a delayed co-condensation synthesis was used to functionalize the outer surface (red dots), followed by template extraction and grafting of the second functional group (in green). The last step proceeded with limited success, mostly enriching the outer CMS surface instead of the internal one. (b) Approach B1 shows a multistep co-condensation synthesis, achieving first the inner surface functionalization (green dots) and then the outer surface functionalization (red dots), by a delayed addition of the second trialkoxysilane. (c) Approach B2 was also applied to obtain aminopropyl groups inside the core of the nanoparticle together with phenyl groups (green and red dots). The functionalized core and shell regions could also be separated from each other by inserting additional thin layers of unfunctionalized mesoporous silica (blue dots).

2.2. Synthesis of CMS by Multistep Co-condensation: Approach B. Two slightly different approaches (namely B1 and B2) were used in this case, as will be further discussed, due to the synthetic difficulties imposed by the co-condensation with aminopropyl groups.

2.2.1. Approach B1: CMS(B)-Ph_{IN}-NH_{OUT}. Solution 1 was prepared with 14.3 g of TEA (95.6 mmol), 1.557 g of TEOS (7.84 mmol, 85 mol % of the total amount of required TEOS), and 110.8 mg (0.461 mmol, 5 mol % of the total TEOS) of phenyltriethoxysilane (PTES, Aldrich, 98%), followed by heating for 20 min at 90 °C without stirring. Meanwhile, 2.41 mL (7.29 mmol) of CTAC and 21.7 g of water (solution 2) were preheated at 60 °C, added to solution 1, and stirred at 500 rpm for 20 min. Next 183.2 mg of TEOS (0.922 mmol, 10 mol % of the total TEOS) was added at one time, and the resulting solution was stirred for an additional 40 min (Figure 2b, first step). After that time, a 1:1 mixture of TEOS and APTES (the outer functionalizing component) was added, using 16.53 mg of APTES (0.0922 mmol, 1 mol % of the total TEOS) and 18.32 mg (0.0922 mmol) of TEOS (Figure 2b, second step); the reaction was then left to stir overnight at room temperature. The sample CMS(B)-Ph_{IN}-NH_{OUT} was then centrifuged, redispersed in EtOH, and extracted (see details below).

2.2.2. Approach B2: CMS(B)-$(Ph/NH)_{IN}$. Solution 1 was prepared with 14.3 g of TEA (95.6 mmol), 1.466 g of TEOS (7.37 mmol, 80 mol % of the total amount of required TEOS), 110.8 mg of PTES (0.461 mmol, 5 mol % of the total TEOS), and 82.65 mg (0.461 mmol) of APTES, followed by heating for 20 min at 90 °C without stirring. Meanwhile, 2.41 mL (7.29 mmol) of CTAC and 21.7 g of water (solution 2) were preheated at 60 °C, added to solution 1, and stirred at 500 rpm for 20 min (Figure 2c, first step). Next 183.2 mg of TEOS (0.922 mmol, 10 mol % of the total TEOS) was added in four increments every 3 min (45.8 mg each) using an Eppendorf micropipet, and the resulting solution was stirred overnight at room temperature (Figure 2c, second step). The sample CMS(B)-$(Ph/NH)_{IN}$ was then centrifuged, redispersed in EtOH, and extracted.

2.3. Template Extraction. Extraction of the organic template from the mesoporous silica nanoparticles was performed by heating the colloidal suspension for 45 min under reflux (90 °C) in a solution containing 2 g of ammonium nitrate in 100 mL of absolute ethanol, followed by 45 min under reflux in a solution of 10 mL of concentrated hydrochloric acid and 90 mL of absolute ethanol. The CMS nanoparticles were then separated by centrifugation (19 000 rpm, 43.146 RCF, 30 min). The material was washed with ethanol after each extraction step. CMS materials were then redispersed in 5 mL of ethanol, obtaining clear ethanolic colloidal suspensions.

2.4. CMS Inner Surface Post-grafting. Samples synthesized with approach A (CMS(A)-Cl_{OUT} and CMS(A)-NH_{OUT}), after extraction, were post-functionalized with trialkoxysilane in order to obtain particles with complementary inside and outside functionalization. The following functionalized trialkoxysilanes were used as inner functionalizing agents: APTES for sample CMS(A)-Cl_{OUT}, and Cl-PTES for sample CMS(A)-NH_{OUT}, thus obtaining, respectively, the samples CMS(A)-NH_{OUT}-Cl_{IN} and CMS(A)-Cl_{OUT}-NH_{IN}.

To achieve an inner functionalization of approximately 5 molecules/nm^2, 0.5 mmol of RTES reagent is needed, according to the following calculation. Considering a total amount of 50 mg of extracted CMS with a surface area of ~1200 m^2/g, 3×10^{20} molecules are needed to have 5 molecules/nm^2, or 0.498 mmol. To achieve a lower functionalization density of the inner surface, 0.25 mmol of the respective functionalized trialkoxysilane was used.

The extracted CMS nanoparticles in ethanol suspension were added to absolute ethanol in a dry flask. After addition of 0.5 mmol of the respective functionalized trialkoxysilane, the reaction mixture was stirred for 4 h under reflux conditions (Figure 2a, third step).

The mixture was then centrifuged and the liquid removed. The post-grafted CMS nanoparticles were redispersed in 5 mL of ethanol.

2.5. Fluorescein Isothiocyanate Labeling. Fluorescein isothiocyanate (FITC, Fluka, ≥90%) labeling was performed, following ref 23, on the bifunctionalized CMS nanoparticles synthesized with approach B, in order to carry out fluorescence quenching experiments with gold nanoparticles.

A total of 85 mg of amino-functionalized CMS (about 10 mL of ethanolic colloidal suspension, depending on the sample concentration) was added to a 10 mL solution of FITC in EtOH. The amount of FITC was a 1.5-fold excess with respect to the molar amount of aminopropyl groups on the CMS (1% for sample CMS-Ph_{IN}-NH_{OUT} and 5% for sample CMS-Ph-NH_{IN}). Sample CMS-Ph_{IN}-NH_{OUT} was also labeled with half of the FITC amount.

The suspension was stirred in the dark for 24 h at room temperature, and then the yellow-colored nanoparticles were collected by centrifugation (19 000 rpm for 20 min), washed two times with EtOH, and finally redispersed in 5 mL of absolute ethanol.

2.6. Synthesis of Dodecanethiolate Gold Nanoparticles. The synthesis of dodecanethiolate-stabilized gold nanoparticles (AuNPs) followed a standard procedure.[24,25] An amount of 0.75 g of tetraoctylammonium bromide ($N(C_8H_{17})_4$, 1.25 equiv, Aldrich, 98%) was vigorously stirred at room temperature in 40 mL of toluene, and a yellow solution of 0.15 g of hydrogen tetrachloroaurate ($HAuCl_4 \cdot 3H_2O$, 0.5 equiv, Sigma, metal basis 99.99%) in 12.5 mL of H_2O was added. Since the $AuCl_4^-$ transferred into the toluene, the organic phase was separated from water, and 0.565 g of dodecanethiol (2.793 mmol, at a ratio RSH:$HAuCl_4 \cdot 3H_2O$ = 7:1, Fluka, ≥97%) was added. The reaction temperature was adjusted to −78 °C (dry ice, acetone), and 0.38 g of sodiumborohydride ($NaBH_4$, 10 equiv, Aldrich, granular, ≥98%) suspended in 25 mL of absolute ethanol was added over a period of 15 min to the stirred $AuCl_4^-$ solution. The reduction step was carried out for 1 h at −78 °C under stirring, and then the solution was warmed slowly to room temperature and additionally stirred for 3 h. The brown organic phase was then collected, the solvent removed in a rotary evaporator, and the black product suspended in 30 mL of ethanol to dissolve the byproducts and sonicated. Finally, the dodecanethiolate-stabilized gold nanoparticles were washed on a glass filtration frit with 80 mL of EtOH and 150 mL of acetone and redispersed in toluene. The final concentration of AuNPs in toluene was 5.65 mM (determined by weighing, after drying in vacuum, a known volume of AuNPs colloidal suspension).

2.7. Characterization. All CMS samples were characterized by nitrogen sorption measurements, performed on a Quantachrome Instruments NOVA 4000e at 77 K. Pore size and volume were calculated using a NLDFT equilibrium model of N_2 on silica. In order to remove the contribution of interparticle mesoporosity, pore volumes were calculated only up to a pore size of 8 nm. A BET model was used to estimate the surface area.

Dynamic light scattering and zeta potential measurements were performed on a Malvern Zetasizer-Nano instrument equipped with a 4 mW He−Ne laser (633 nm) and avalanche photodiode detector. DLS measurements were directly recorded on the ethanolic suspension. For the determination of the zeta potential profiles, one drop of the ethanolic suspension (∼3 wt %) was mixed prior to measurement with 2 mL of commercial Hydrion Buffer solution, having pH values of 2, 3, 4, 5, and 6.

Thermogravimetric analyses of the bulk samples (about 10 mg of dried powder) were performed on a Netzsch STA 440 Jupiter thermobalance (heating rate of 10 K/min in a stream of synthetic air of about 25 mL/min).

TEM samples were prepared by adding 3 drops of the ethanolic CMS suspension (∼3 wt %) to 4 mL of absolute EtOH and drying of a drop of the resulting diluted colloidal suspension on a carbon-coated copper grid.

Fluorescent spectra were recorded with a PTI spectrofluorometer with a photomultiplier detection system (model 810/814). The FITC-labeled CMS samples were dispersed in EtOH (13.2 nM with respect to the total amount of FITC-label, based on reactant stoichiometry), and 3 mL of this diluted ethanolic suspension was measured (λ_{ex}= 450 nm) in a 1 cm quartz cuvette (QG Hellma) in a cuvette holder with magnetic stirring. Since the sample CMS(B)-$(Ph/NH)_{IN}$ shows a concentration of 5% molar (relative to total Si) of aminopropyl groups and sample CMS(B)-Ph_{IN}-NH_{OUT} 1% molar, the amount of CMS nanoparticles dispersed into the ethanolic solution for the fluorescence measurement was adjusted in order to have the same concentration of FITC groups: thus, 0.265 μM CMS(B)-$(Ph/NH)_{IN}$ and 1.314 μM CMS(B)-Ph_{IN}-NH_{OUT} (based on reactant stoichiometry).

To quench the fluorescence intensity of FITC-labeled CMS nanoparticles, toluene suspensions of AuNPs having different concentrations (solution 1, 5.64 nM; solution 2, 5.64 μM; solution 3, 5.64 mM) were gradually added to the 3 mL solution in the cuvette, starting from the solution with the lowest concentration (for solution 1, 10 μL each up to 500 μL; then for solution 2, 10 μL each up to 100 μL; finally for solution 3, 2.5 μL each up to 20 μL). After quenching, cyanide anions were added, which are known to form strong complexes with gold and to displace the more weakly bound ligand FITC from the AuNPs. Thus, 10 μL of a KCN solution in water (0.1 M) was added three times into the cuvette containing FITC-labeled CMS and AuNPs. The following increase of the fluorescence emission spectra, due to the nonquenched FITC, was then recorded.

Absorption spectra of the FITC-labeled CMS during the quenching experiment with AuNPs suspensions were also recorded on a Hitachi U-3501 UV−vis spectrophotometer to examine the possibility that the quenching of the FITC fluorescence could be attributed to the absorption of the AuNPs.

3. Results and Discussion

3.1. Characterization of the CMS Synthesized by Approach A. The first approach used to achieve bifunctionalized CMS nanoparticles combined a delayed co-condensation step of the nanoparticles to enrich the outer surface with a selected trialkoxysilane group and, after the template extraction, a post-grafting approach to functionalize the internal mesopores with another trialkoxysilane moiety. In the present work, the outer surface is defined as the external shell of the CMS nanoparticles, whereas the inner surface refers to the mesopore walls in the inner core of the CMS nanoparticles.

CMS materials were synthesized on the basis of the insights gained in our previous research[8,11] by hydrolyzing TEOS in a mixture of CTAC and TEA, which leads to high nucleation rates and slow growth of the generated seeds (Figure 2a, first step). After about 30 min into the synthesis, it was shown[11] that the seeds already formed mesoporous silica nanoparticles that can react with additional reagents. The subsequent addition of small amounts of a trialkoxysilane (RTES) (1% of the total amount of silane content) in combination with TEOS (RTES:TEOS = 1:1) allows us to functionalize the outer shell of the grown nanoparticles (Figure a, second step).

By using (3-chloropropyl)trimethoxysilane and (3-aminopropyl)trimethoxysilane for the above procedure, the samples CMS(A)-Cl_{OUT} and CMS(A)-NH_{OUT} were respectively synthesized and then the template was extracted. Thermogravimetic

(23) Salmio, H.; Bruehwiler, D. *J. Phys. Chem.* **2007**, *111*, 923–929.
(24) Hostetler, M. J.; Wingate, J. E.; Zhong, C.-J.; Harris, J. E.; Vachet, R. W.; Clark, M. R.; Londono, J. D.; Green, S. J.; Stokes, J. J.; Wignall, G. D.; Glish, G. L.; Porter, M. D.; Evans, N. D.; Murray, R. W.; Royce, W. *Langmuir* **1998**, *14*, 17–30.
(25) Brust, M.; Walker, M.; Bethell, D.; Schiffrin, D. J.; Whyman, R. *J. Chem. Soc., Chem. Commun.* **1994**, 801–802.

analysis data, showing the amount of functionalizing agent, and structural data obtained by nitrogen sorption measurements are reported in the Supporting Information (Figure S-1 and Table S-1). Zeta potential measurements confirmed the presence of the aminopropyl group on the outer surface of the CMS(A)-NH_{OUT} nanoparticles (Figure S-3.a), since they carry a positive charge, being protonated at acidic pH values. In contrast, since the chloropropyl groups are uncharged at high or low pH values, the zeta potential curve of sample CMS(A)-Cl_{OUT} (Figure S-3b) is similar to that of the unfunctionalized CMS.

In order to enrich the inner surface with a second functional group in the already shell-functionalized nanoparticles (CMS(A)-Cl_{OUT} and CMS(A)-NH_{OUT}), a post-grafting approach was applied (Figure 2a, third step). The two resulting types of nanoparticles can be considered as complementary: (i) the chloropropyl groups grafted only onto the internal pore surface and the amino groups on the outer shell (sample CMS(A)-NH_{OUT}-Cl_{IN}), and vice versa (ii) the aminopropyl groups only in the mesopores and the Cl groups on the external particle surface (sample CMS(A)-Cl_{OUT}-NH_{IN}). However, the zeta potential measurement did not confirm the localization of the two functional groups into separate zones of the CMS nanoparticles, i.e., the inner and outer surfaces, respectively. If the post-grafting functionalized only the inner surface of the nanoparticles, then the outer surface, already functionalized by aminopropyl groups, would remain unmodified by the post-grafting, and the zeta potential curve values should have remained unaffected, in contrast to the observed behavior shown in Figure S-3. These results are explained by assuming that, while the co-condensation step ensured a high degree of functionalization of the outer surface of the particles, some free silanol groups still remained because a mixture 1:1 of TEOS and RTES was used. When the post-grafting step was applied, these silanols were more easily functionalized than the internal silanols in the mesopores, since the access to the silanols on the inner surface is limited by diffusion resistance.[26] It was concluded that another approach avoiding the post-grafting step would be required.

3.2. Characterization of the CMS Synthesized by Approach B. An alternative multistep co-condensation approach was conceived, based on delayed co-condensation synthesis, in order to precisely localize the functional groups in the inner pore surface or on the outer shell of the CMS nanoparticles (Figure 2b,c). In particular, the two functional groups PTES and APTES were used: phenyl groups were maintained in the internal core of the nanoparticle as a constant feature, whereas the position of the aminopropyl groups was varied, i.e., inside or at the periphery of the CMS nanoparticle. Thus, for amino functionalization on the outer shell of the nanoparticle, a delayed co-condensation approach was applied, as described in the Experimental Section and in Figure 2b: 20 min after the initial co-condensation of TEOS and PTES, a layer of silica was precipitated around the core (first step), and after an additional 40 min another shell-layer of TEOS and APTES was synthesized (second step), obtaining the sample CMS(B)-Ph_{IN}-NH_{OUT}.

In contrast, to maintain the aminopropyl groups in the internal core of the CMS nanoparticles (Figure 2c), simultaneous co-condensation of TEOS with PTES and APTES was performed (first step), and 20 min later a layer of TEOS was applied (second step) with the aim to isolate the internally functionalized core from the external environment. The sample code is CMS(B)-$(Ph/NH)_{IN}$.

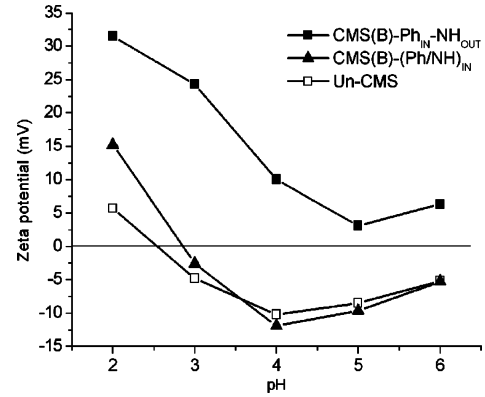

Figure 3. Zeta potential of CMS samples prepared by approach B: Un-CMS (□), CMS having the amino functionality in the internal core (CMS(B)-$(Ph/NH)_{IN}$, ▲), and CMS with outer shell functionalized with aminopropyl groups (CMS(B)-Ph_{IN}-NH_{OUT}, ■).

We will elaborate on the rationale for introducing phenyl groups into the core of the CMS(B)-$(Ph/NH)_{IN}$ nanoparticles. The reason, widely described in the literature,[27−30] lies in the difficulties in synthesizing a mesoporous system by a co-condensation approach using aminopropyl-alkoxysilane as reagent. The lack of organized mesoporosity in the case of co-condensed amino-functionalized SBA-15 materials was already observed:[27,28] apparently the protonation of APTES in acidic mixtures has a disruptive effect on the formation of SBA-15 mesostructure, even at relatively low concentrations. In contrast, the use of phenyl groups in combination with aminopropyl groups leads to a well-ordered mesoporous structure and increases the stability of the mesoporous phase.[9]

The additional silica shell made of pure TEOS was synthesized around the inner core of the particles in both approaches B1 and B2 with the aim to (i) to separate the inner core functionalities from the outer shell of aminopropyl groups, in the case of CMS(B)-Ph_{IN}-NH_{OUT} sample, approach B1, and (ii) to create a barrier between the functionalized inner core and the external medium. In approach B2, a multistep addition of TEOS was performed to give the silica source enough time to organize itself around the already-formed functionalized core, enriching the outer surface of the nanoparticle with unfunctionalized mesoporous silica. The presence of phenyl groups was confirmed by Raman spectroscopy (see the Supporting Information, Figure S-6).

The degree of template removal by extraction was determined by Raman spectroscopy (Figure S-6) and TGA, evaluating the remaining cetyltrimethylammonium template in the range from 110 to about 395 °C. We observe a weight loss of 8−10 wt % due to the residual surfactant in the core−shell extracted samples, i.e., CMS-$(Ph/NH)_{IN}$ and CMS-Ph_{IN}-NH_{OUT}.

The different localization of the aminopropyl groups in the extracted samples was examined with zeta potential measurements (Figure 3). The curve related to the CMS(B)-Ph_{IN}-NH_{OUT} sample, having the amino functionalities displaced on the outer

(26) Shephard, D. S.; Zhou, W.; Maschmeyer, T.; Matters, J. M.; Roper, C. L.; Parsons, S.; Johnson, B. F. G.; Duer, M. J. *Angew. Chem., Int. Ed.* **1998**, *37*, 2719–2723.

(27) Chong, A. S. M.; Zhao, X. S.; Kustedjo, A. T.; Qiao, S. Z. *Microporous Mesoporous Mater.* **2004**, *72*, 33–42.

(28) Wei, Q.; Nie, Z.-R.; Hao, Y.-L.; Liu, L.; Chen, Z.-X.; Zou, J.-X. *J. Sol-Gel Sci. Technol.* **2006**, *39*, 103–109.

(29) Burkett, S. L.; Sims, S. D.; Mann, S. *Chem. Commun.* **1996**, 1367–1368.

(30) Macquarrie, D. J. *Chem. Commun.* **1996**, *16*, 1961–1962.

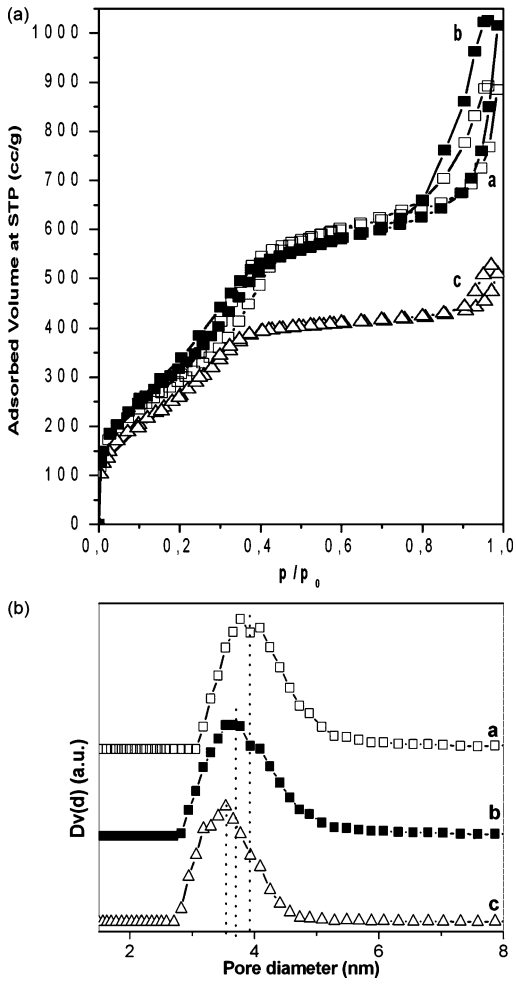

Figure 4. (a) Nitrogen sorption isotherms and (b) DFT pore size distributions of the CMS samples synthesized with approach B: Un-CMS (curve a, □), CMS(B)-Ph_{IN}-NH_{OUT} (curve b, ■), and CMS(B)-$(Ph/NH)_{IN}$ (curve c, △).

Table 1. Structural Parameters from Nitrogen Sorption Isotherms of the Bifunctionalized CMS Nanoparticles Synthesized with Approach B in a Multistep Co-condensation Synthesis

sample	DFT pore size (nm)	pore volume (cm^3/g)	BET surface area (m^2/g)
(a) Un-CMS	3.77	0.857	1314
(b) CMS(B)-Ph_{IN}-NH_{OUT}	3.65	0.772	1302
(c) CMS(B)-$(Ph/NH)_{IN}$	3.54	0.601	1059

shell of the particles, shows a surface with high positive charge. In contrast, the behavior of CMS(B)-$(Ph/NH)_{IN}$, with aminopropyl groups in the particle core, is very similar to that of unfunctionalized CMS, thus confirming that the amino functionalities located in the inner core of the CMS do not affect the external charge of the nanoparticles.

Nitrogen sorption measurements show that both bifunctionalized samples are mesoporous, with high surface area and pore volume (Figure 4 and Table 1). Slightly smaller values can be observed for the CMS(B)-$(Ph/NH)_{IN}$ sample with respect to the CMS(B)-Ph_{IN}-NH_{OUT} nanoparticles; this is attributed to the presence of two functional groups in the mesopore system at a molar ratio of 10% of the total amount of silane. In general, a decrease of the maximum in the DFT pore size distribution (Figure 4b) is observed with respect to sample Un-CMS, since the mesopores are modified at high density with one group (phenyl) or two groups (phenyl and aminopropyl).

Evidence for the mesoporous and non-aggregated nature of the CMS nanoparticles is shown with TEM, showing no structural differences between the unfunctionalized CMS (Figure 5a) and the multiple core−shell functionalized ones (CMS(B)-Ph_{IN}-NH_{OUT} in Figure 5b and CMS(B)-$(Ph/NH)_{IN}$ in Figure 5c).

3.4. Characterization of Core−Shell FITC-Labeled CMS. As described above, zeta potential measurements already provide significant evidence for the successful localization of the aminopropyl functional groups in the CMS nanoparticles. Here we describe an additional experimental technique based on fluorescence quenching that serves to elucidate the localization of the different functional groups. Fluorescein isothiocyanate (FITC) is a versatile labeling reagent, forming a thiourea linkage upon reaction with the aminopropyl group (Figure 6a). This labeling concept was applied to both samples CMS(B)-$(Ph/NH)_{IN}$ and CMS(B)-Ph_{IN}-NH_{OUT}, effectively using the FITC distribution as a sensor for the underlying distribution of the amino groups in the respective nanoparticles (Figure 6b).

The reaction of FITC with aminopropyl groups located at the internal surface is expected to give a reduction of the pore size distribution (Figure 7a and Table 2), as already reported in the literature,[23] whereas the coupling of FITC with aminopropyl groups anchored to the external surface should have no such effect (Figure 7b). In general, a reduction of the pore volume and the BET surface area is observed for all samples (Table 2). From TGA, the calculated amount of grafted FITC is 0.145 and 0.036 mmol/g for samples CMS(B)-$(Ph/NH)_{IN}$-FITC and CMS(B)-Ph_{IN}-NH_{OUT}-FITC, respectively (for further details, see Supporting Information, Figure S-7 and Table S-2).

The fluorescence spectra of the two FITC-labeled CMS (Figure 8) show for both samples (CMS(B)-Ph_{IN}-NH_{OUT}-FITC, solid line; CMS(B)-$(Ph/NH)_{IN}$-FITC, empty triangles) an emission at 519 nm and an additional emission at 550 nm only for the sample CMS(B)-Ph_{IN}-NH_{OUT}. The latter emission is attributed to the formation of J-aggregates, and it is red-shifted with respect to the emission of the dye monomer.[31] The J-band has been attributed to a delocalized coherent excitonic state caused by head-to-tail alignment of transition dipoles of the dye,[32] associated with a high concentration of FITC molecules, in the present case at the outer surface of the CMS(B)-Ph_{IN}-NH_{OUT} nanoparticles.

To avoid the formation of the J-band, sample CMS(B)-Ph_{IN}-NH_{OUT} was then labeled with half of the amount of FITC used before. As expected, the emission spectrum in Figure 8 related to this sample (CMS(B)-Ph_{IN}-NH_{OUT}-$^1/_2$FITC, dashed line) shows the emission peak at 519 nm but the absence of the J-band, since a lower density of FITC molecules was present on the outer surface of the CMS nanoparticles. A slight reduction in the intensity of the emission spectrum can be observed with respect to the other samples, due to the lower amount of FITC label. We also note that, after FITC labeling with the reduced amount, the nitrogen sorption isotherm of the sample CMS(B)-Ph_{IN}-NH_{OUT}-$^1/_2$FITC (Figure 7b, ○) shows a slightly higher N_2 adsorbed volume with respect to the sample labeled with the full amount of FITC (CMS(B)-Ph_{IN}-NH_{OUT}-FITC, ●). The values of pore volume and surface area of the sample CMS(B)-Ph_{IN}-NH_{OUT}-$^1/_2$FITC are also between those of CMS(B)-Ph_{IN}-

(31) *J-aggregates*; Kobayashi, T., Ed.; World Scientific: Singapore, 1996.
(32) Kitahama, Y.; Yago, T.; Furube, A.; Katoh, R. *Chem. Phys. Lett.* **2008**, *457*, 427–433.

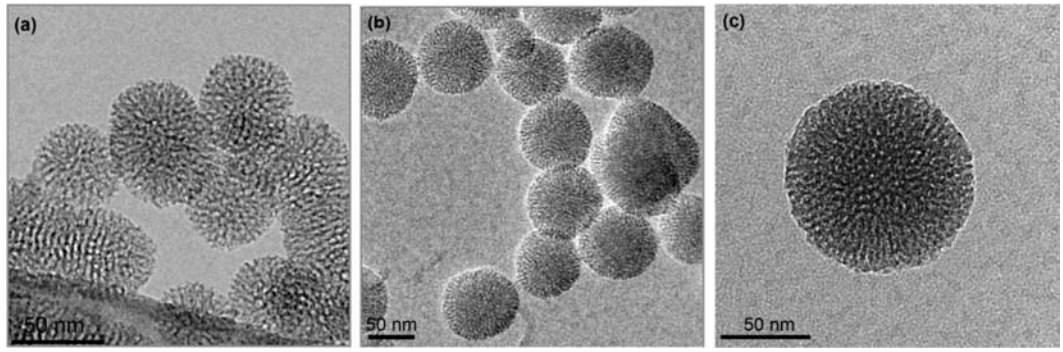

Figure 5. Transmission electron micrographs of CMS nanoparticles: (a) Un-CMS, (b) CMS(B)-Ph_{IN}-NH_{OUT}, and (c) CMS(B)-$(Ph/NH)_{IN}$.

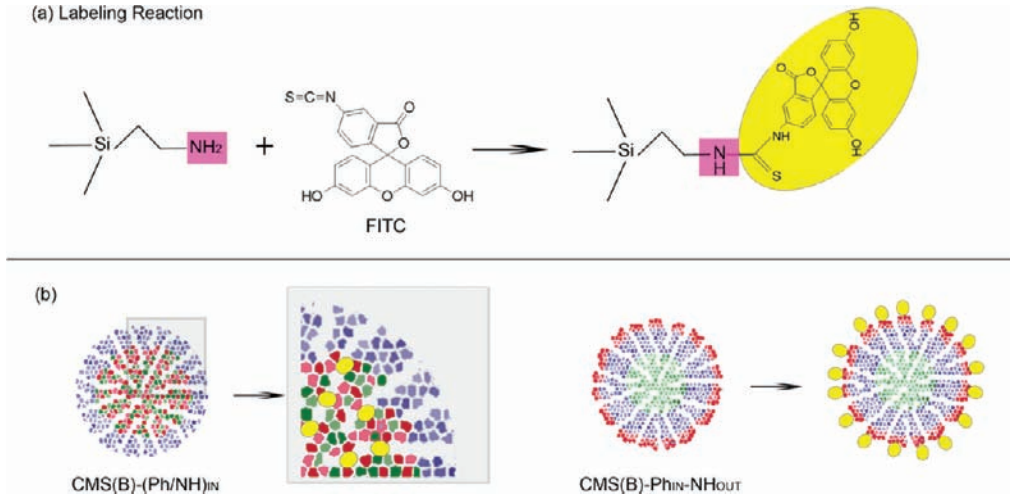

Figure 6. (a) Reaction scheme between the aminopropyl groups of the CMS nanoparticle and fluorescein isothiocyanate (FITC). (b) Localization of the FITC-labeled amino groups into the two bifunctional samples.

NH_{OUT} and the CMS(B)-Ph_{IN}-NH_{OUT}-FITC (Table 2), thus confirming that a lower FITC density on the external particle surface has been achieved.

3.5. Quenching Experiments with AuNPs. Quenching experiments with dodecanethiolate-stabilized gold nanoparticles (AuNPs) were conceived in order to determine the localization of the aminopropyl functionality through the localization of the FITC label.

AuNPs were prepared according to a modified procedure reported in the literature,[24] by tuning the synthesis parameters to obtain a colloidal suspension with AuNPs of about 4 nm in diameter. TEM characterization (see Supporting Information, Figure S-8) shows the inner metal core of AuNPs having an average diameter of about 3 nm.

Three solutions of colloidal AuNPs in toluene having different concentrations were prepared (SOL1, 5.65 nM; SOL2, 5.65 μM; SOL3, 5.65 mM) in order to gradually quench the fluorescence emission of the FITC-labeled CMS nanoparticles.

Figure 9 shows the emission spectra of the FITC-labeled nanoparticles at the beginning (filled line) and after each addition of AuNPs-SOL1 (dotted line), then of SOL2 (dashed line), and finally of SOL3 (empty circles). Details of these subsequent additions are reported in the Experimental Section and in Table S-3 in the Supporting Information. For clarity, some curves have been omitted.

We observe that, upon addition of the AuNPs, a gradual reduction of the fluorescence emission is observed for the CMS(B)-Ph_{IN}-NH_{OUT} samples, having full (Figure 9a,b) or half the amount (Figure 9c) of labeled FITC, whereas no influence on the fluorescence spectra after introducing the AuNPs solutions is noticeable for the CMS(B)-$(Ph/NH)_{IN}$-FITC sample (Figure 9d). The latter experiment also clearly demonstrates that, at the given concentrations, the introduction of the AuNPs solution per se does not reduce the fluorescence intensity due to absorption. The fluorescence emission of the dye can be quenched through transfer of the excitation energy to another molecule or to a metal surface. At small molecule−metal separations, the collective excitations in the metal, such as surface plasmon and electron−hole pair excitations, can act as energy acceptors. The electron gas of the metal will dissipate this energy into the bulk through various scattering processes. This mechanism is effective over distances less than about 8 nm.[33,34] The results shown in Figure 9 clearly show that the energy transfer between the FITC molecules and the gold particles is possible only at small distances, thus only when FITC is attached to the outer surface of the CMS nanoparticles (samples CMS(B)-Ph_{IN}-NH_{OUT}-FITC and CMS(B)-Ph_{IN}-NH_{OUT}-$^1/_2$FITC). In the case of FITC-labeling into the nanoparticle core (sample CMS(B)-$(Ph/NH)_{IN}$-FITC) no quenching is observed, due to the distance between the gold quencher and the fluorescent dye molecules. The unfunctionalized mesoporous silica shell around the functional core of the sample CMS(B)-

(33) *Photoluminescence of Solutions*; Parker, C. A.; Ed.; Elsevier: Amsterdam, 1968.
(34) Whitmore, P. M.; Robota, H. J.; Harris, C. B. *J. Chem. Phys.* **1982**, *77*, 1560–1568.

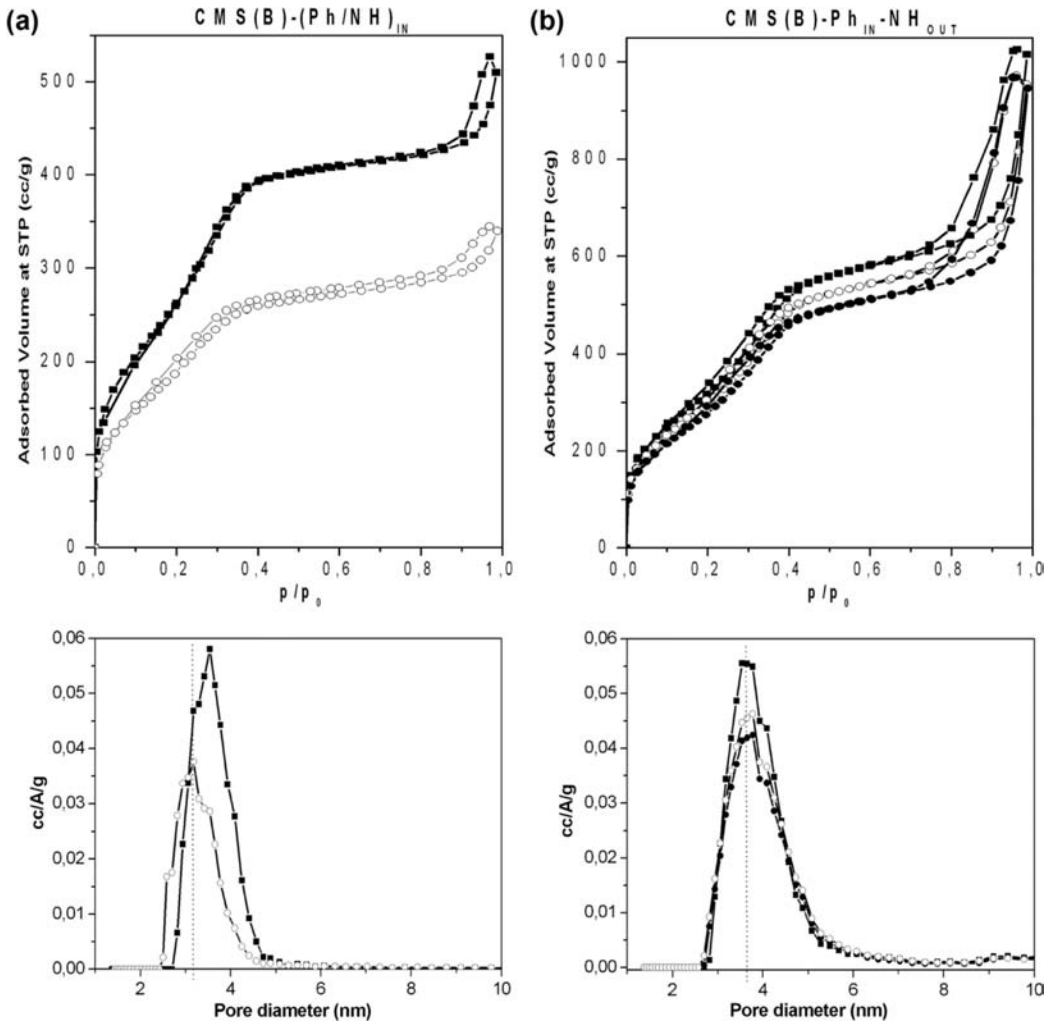

Figure 7. Nitrogen sorption measurements and DFT pore size distributions for samples: (a) CMS(B)-$(Ph/NH)_{IN}$ before (■) and after FITC labeling (○); (b) CMS(B)-Ph_{IN}-NH_{OUT} before (■), and after FITC labeling: CMS(B)-Ph_{IN}-NH_{OUT}-$^1/_2$FITC (○) and CMS(B)-Ph_{IN}-NH_{OUT}-FITC (●).

Table 2. Structural Parameters for the CMS Nanoparticles after FITC Labeling

sample	DFT pore size (nm)	pore volume (cm^3/g)	BET surface area (m^2/g)
CMS(B)-$(Ph/NH)_{IN}$	3.54	0.601	1059
CMS(B)-$(Ph/NH)_{IN}$-FITC	3.18	0.507	781
CMS(B)-Ph_{IN}-NH_{OUT}	3.65	0.772	1302
CMS(B)-Ph_{IN}-NH_{OUT}-$^1/_2$FITC	3.65	0.730	1261
CMS(B)-Ph_{IN}-NH_{OUT}-FITC	3.65	0.660	1162

$(Ph/NH)_{IN}$ imposes a large distance between the FITC-labeled aminopropyl groups and the AuNPs, which, due to their dimensions, are prevented from diffusing into the mesopores.

In reference experiments, the colloidal AuNPs were also introduced into an ethanolic solution of free FITC. The corresponding fluorescence emission spectra (excitation at 450 nm, 13.2 nM in FITC, see Supporting Information, Figure S-9) show a quenching behavior similar to that of the mesoporous nanoparticles with FITC at their outer surface.

Additional UV−vis absorption spectra have been recorded on the same solutions during the quenching experiments for all the three samples at each AuNPs addition (see Supporting Information, Figure S-10). The results show a very low absorbance in the wavelength range of interest for the fluorescence-quenching experiments. A significant reduction in fluorescence intensity can thus be attributed to the energy transfer between the FITC and the AuNP plasmon band, and not to the absorption of the light emitted by the gold nanoparticles.

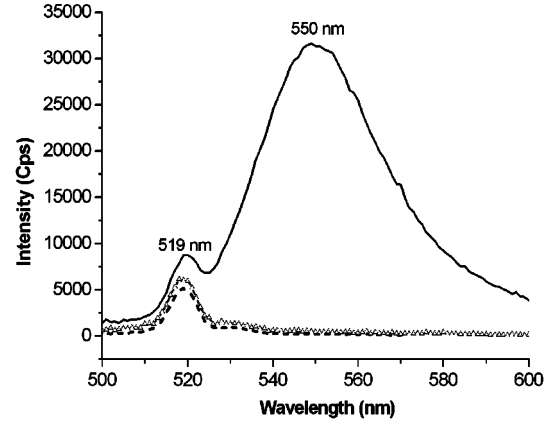

Figure 8. Fluorescence emission spectra (excitation at 450 nm) for fluorescein-labeled samples: CMS(B)-Ph_{IN}-NH_{OUT}-FITC (solid line), CMS(B)-$(Ph/NH)_{IN}$-FITC (empty triangle), and CMS(B)-Ph_{IN}-NH_{OUT}-1/2FITC (dashed line).

These results clearly show that the delayed co-condensation strategy results in multiple core−shell particles with differential localization of various molecular functionalities.

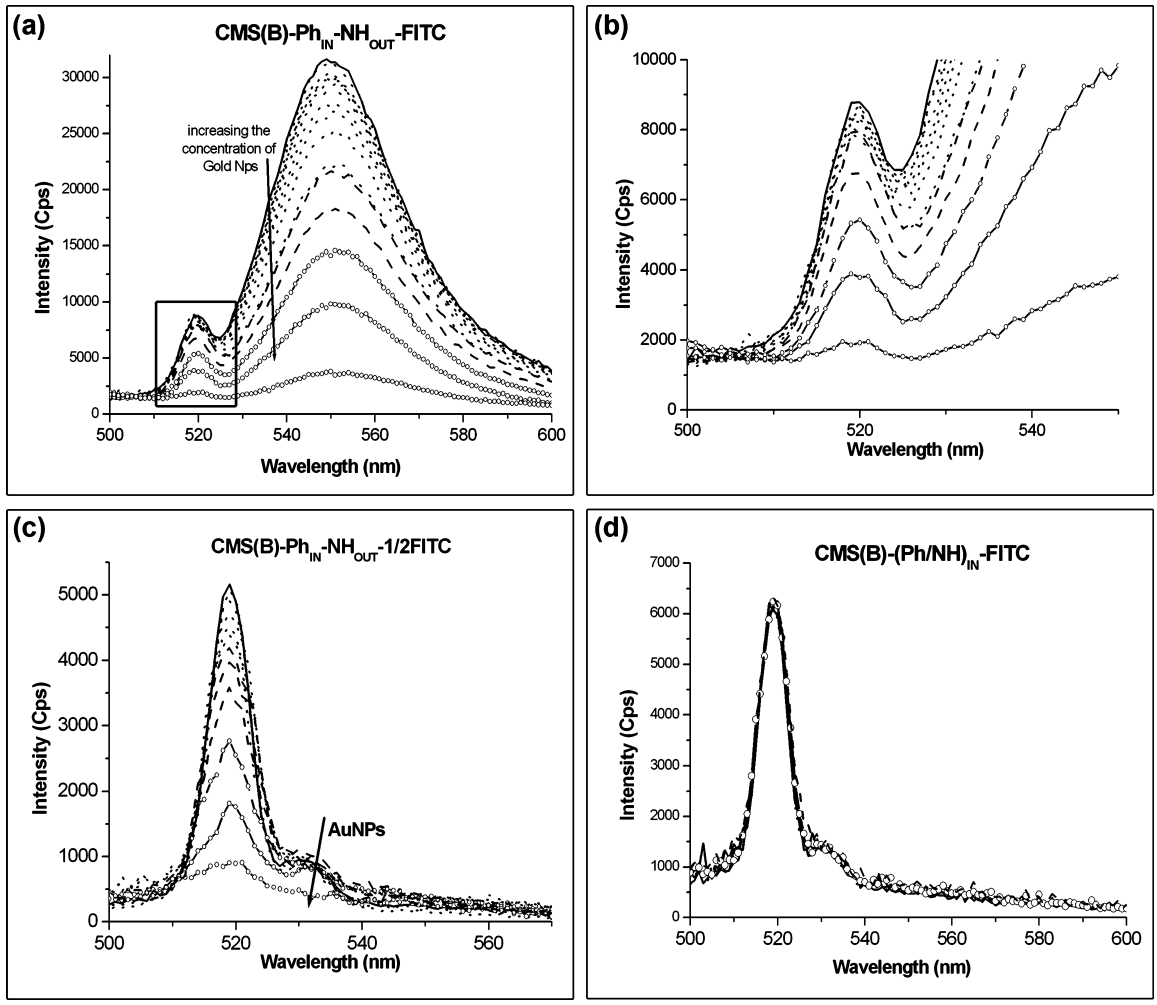

Figure 9. Fluorescence emission spectra (excitation at 450 nm) for FITC-labeled CMS samples (filled lines): (a) CMS(B)-Ph$_{IN}$-NH$_{OUT}$-FITC; (b) inset magnification in the range 500−550 nm; (c) CMS(B)-Ph$_{IN}$-NH$_{OUT}$-$^1/_2$FITC; (d) CMS(B)-(Ph/NH)$_{IN}$-FITC and their fluorescence quenching with AuNps: SOL1 (dotted line), SOL2 (dashed line), or SOL3 (empty circles). For clarity, not all the quenched fluorescence spectra are shown. In particular, in (a), (b) and (d) we report the following amounts of added AuNP solutions: for SOL1 (5.64 nM) 10, 30, 50, 75, 100, 150, 200, 300, 500 μL; for SOL2 (5.64 μM) 20 and 50 μL; for SOL3 (5.64 mM) 5, 10, and 20 μL. In (c) we show the following added volumes of AuNP solutions: for SOL1 (5.64 nM) 30, 50, 100, 200, and 500 μL; for SOL2 (5.64 μM) 10, 20, and 50 μL; for SOL3 (5.64 mM) 2.5, 10, and 20 μL.

Moreover, we have performed additional measurements aimed at the controlled removal of the AuNPs from the mesoporous silica nanoparticles, by adding cyanide ions into the quenched-FITC-labeled CMS. It was already reported in the literature[35] that the formation of a strong cyanide complex with gold ($Au(CN)_2^-$) can remove it from the interaction with FITC. If this approach is correct, one would expect, after the addition of CN^- anions, an increase of the fluorescence intensity of the liberated FITC molecules on the surface of the mesoporous silica. This is indeed observed (Figure 10) for the sample CMS(B)-Ph$_{IN}$-NH$_{OUT}$-$^1/_2$FITC (gray line), for which, after quenching with AuNPs-SOL3 (empty dot line), the addition of KCN solution (filled squares lines) increases again the fluorescence intensity of the CMS nanoparticles. The increase of the pH, caused by the release of hydroxyl anions during the complexation reaction, is responsible for the broadening of the fluorescence peak, due to the pH-sensitivity of the FITC.

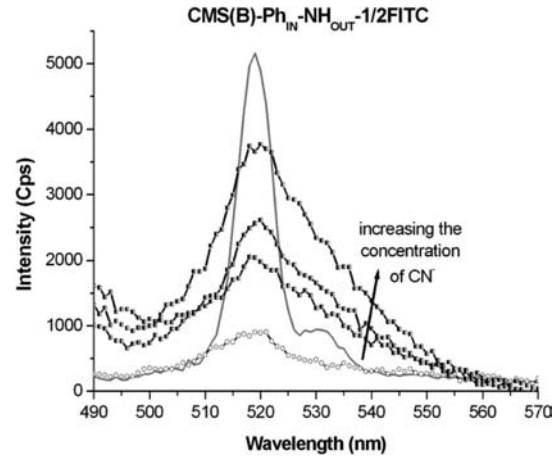

Figure 10. Cyanide anion addition to the quenched solution of sample CMS(B)-Ph$_{IN}$-NH$_{OUT}$-$^1/_2$FITC. Gray line, initial fluorescent solution of the sample; empty dot line, quenched solution with AuNPs-SOL3; filled square lines, subsequent addition of KCN solution (0.1 M) into the cuvette (10, 20, and 30 μL).

(35) *Comprehensive Coordination Chemistry*; Puddephatt-Gold, R. J., Ed.; Pergamon: Oxford, 1987.

4. Conclusions

In the present work we report on the synthesis of multiple core−shell colloidal mesoporous silica (CMS) nanoparticles having two different molecular functionalities in the inner surface and on the outer particle shell. Two different approaches were compared in order to obtain template-free bifunctionalized CMS; in one case a delayed co-condensation approach to functionalize the external shell, followed by template extraction and post-grafting of the internal surface (Approach A), whereas the second method involves different co-condensation steps in order to achieve the bifunctionalization of the CMS in a multistep co-condensation synthesis, followed by template extraction (approach B). The samples were prepared with a complementary design: CMS nanoparticles having a functional group X in the inner core and another functional group Y on the outer shell (CMS-X_{IN}-Y_{OUT}) were compared with their counterparts, having the groups X and Y in the inner surface of the mesopores (CMS-$(X/Y)_{IN}$).

The greatest control over localization of functionality was achieved in a multistep synthesis based on several delayed co-condensation steps (approach B). Several techniques were employed to confirm the distinct localization of functionality in these mesoporous nanoparticles, i.e., nitrogen sorption, zeta potential measurements, and fluorescence spectroscopy. In particular, fluorescence quenching (with gold nanoparticles) of fluorescein isothiocyanate (FITC) attached to aminopropyl functional groups in different shells of the particles provides high-resolution information on localization. We show that the energy transfer between grafted FITC molecules and AuNP plasmons is possible only when the dye is located close to the metal nanoparticles, i.e., on the outer surface of the mesoporous CMS particles.

In general, our delayed co-condensation approach thus allows us to synthesize various bifunctional mesoporous nanoparticles with controlled localization of different functional groups in the inner core or on the outer shell of the nanoparticles. This strategy opens the door for the design of numerous highly functionalized porous nanoparticles, with applications including controlled drug delivery, catalysis, and chemical sensing.

Acknowledgment. Support from DFG-SFB 486 and from the NIM Cluster (LMU München) is gratefully acknowledged.

Supporting Information Available: Further characterization of the CMS systems synthesized by approaches A and B, thermogravimetric results after FITC labeling, characterization of the AuNPs, fluorescence emission spectra of free FITC, and details on quenching experiments (fluorescence emission values at each quenching step and UV−vis absorption spectra). This material is available free of charge via the Internet at http://pubs.acs.org.

JA809346N